Available online at www.sciencedirect.com
ScienceDirect
Journal of Power Sources 175 (2008) 851–860
JOURNAL OF POWER SOURCES
www.elsevier.com/locate/jpowsour

A semi-empirical method for electrically modeling of fuel cell: Executed on a direct methanol fuel cell

Yang Wang [a], G. Au [b], E.J. Plichta [b], J.P. Zheng [a,c,*]

[a] *Department of Electrical and Computer Engineering, Florida A&M University and Florida State University, Tallahassee, FL 32310, United States*
[b] *US Army CERDEC, Fort Monmouth, NJ 07703, United States*
[c] *Center for Advanced Power Systems, Florida State University, Tallahassee, FL 32310, United States*

Received 27 July 2007; received in revised form 27 September 2007; accepted 28 September 2007
Available online 7 October 2007

Abstract

In this paper, a novel semi-empirical modeling method to mathematically derive a nonlinear equivalent circuit from a special group of impedance fuel cell models is proposed. As an example, a 5-cm^2 direct methanol fuel cell (DMFC) was modeled by this method. The derived equivalent circuit is composed of lumped nonlinear resistors, capacitors and an inductor. The nonlinear circuit has an impedance equivalent to the target fuel cell in various operating conditions and provides a good approximation of the static and transient behaviors of the fuel cell. The equivalent circuit fuel cell model was validated by comparing its numerical simulation results with its polarization curve and the dynamic behavior of the target DMFC. These comparisons were performed while the DMFC was operating under square current pulses with different upper and low current levels.
© 2007 Elsevier B.V. All rights reserved.

Keywords: DMFC; Fuel cell model; Impedance; Equivalent circuit; Dynamic behavior

1. Introduction

Recently, research interest in dynamic fuel cell model has increased. Various attempts have been made to model the static and dynamic behaviors of fuel cells. Most of them are physics-based mathematical fuel cell models that consist of multiple time partial differential equations based on electrochemistry, electronics, mechanics, thermal dynamics, fluid dynamics and others. These models directly link the transient phenomena to the intrinsic physical parameters of fuel cell and have high precision in simulating the transient response of fuel cell. The models can accurately predict cell performance with the main purpose of fuel cell design. However, the complex calculations of these models and proprietary nature of some physical parameters in commercial fuel cells retard its use for fuel cell control and fuel cell power system design. Therefore, many reduced-order (or control-oriented) fuel cell models were investigated for such demands, but most of them are still mathematical in nature.

Since most of the intrinsic physical parameters and variables of fuel cells are constrained or controlled in a commercial fuel cell power module, a simpler electric circuit dynamic fuel cell model should be allowed and it will be more helpful to power electronics designer. Several equivalent electric circuit dynamic fuel cell models were published for this purpose [1–5]. Larminie and Dicks introduced a fundamental empirical electric circuit model for fuel cells [1]. The model has two resistors and a capacitor. One of the resistors models the activation polarization and the other models the cell ohmic resistance. These resistors in combination represented the steady-state performance of the fuel cell. A capacitor is connected across the resistor for activation polarization to model the capacitive dynamic behavior of fuel cells. Of course, this resistor–capacitor pair is too simple to represent the complex activation impedance. However, because of its simple configuration, this model was widely referenced by modeling researchers to empirically introduce the cell ohmic resistance and capacitance into their electrochemical fuel cell models. As one kind of electric circuit models, impedance fuel cell models [2] are mapped from the electrochemical impedance

* Corresponding author at: Department of Electrical and Computer Engineering, Florida A&M University and Florida State University, Tallahassee, FL 32310, United States. Tel.: +1 850 410 6464; fax: +1 850 410 6479.
E-mail address: zheng@eng.fsu.edu (J.P. Zheng).
URL: http://www.eng.fsu.edu/~zheng/ (J.P. Zheng).

0378-7753/$ – see front matter © 2007 Elsevier B.V. All rights reserved.
doi:10.1016/j.jpowsour.2007.09.101

spectrum of the fuel cell operating under certain running conditions. These models are linear equivalent circuit fuel cell models that excluded the nonlinearity of the steady-state polarization and low frequency response of fuel cells running in different conditions. Instead, these models are typically used to study the high frequency response of fuel cell such as ripple current due to the interaction of the fuel cell and power converter for a certain operating point [2]. Yu and Yuvarajan published a nonlinear equivalent circuit fuel cell model in which two transistors, a diode and an inductor were included to model the activation polarization as well as concentration polarization. However, it is an empirical equivalent circuit fuel cell model, and was phenomenally derived and limited at a certain electrical operating point [3]. These electric circuit models are not suitable for simulating the fuel cell running in various operating conditions. Though electrochemical circuit fuel cell models [4,5] are also a kind of electric circuit fuel cell models, they are far different from the above circuit models. These electrochemical circuit fuel cell models were developed based on the transformation of the complex differential equations of an electrochemical fuel cell model into a series of electric circuit networks. These models can be directly installed into power electronic design software tools (e.g. PSPICE, MATLAB/SIMULINK). However, these models are still mathematical fuel cell models in nature. In these models, steady-state approximations were used to simplify certain complex differential equations to transform them into electric circuit networks. These approximations neglected lots of electrochemical transient responses except the slow variations of temperature and humidity changes of fuel cells. The other shortcoming of electrochemical circuit models is the use of physics parameters that are hard to be obtained from commercial fuel cells. As a fully functional dynamic fuel cell model for power electronic system design, the preferable nonlinear equivalent circuit model should be available to simulate the static and dynamic behaviors of the fuel cells running under various electrical operation conditions. The parameters of the model should be easily and directly obtained from the target fuel cell.

This paper presents a novel fuel cell modeling method that was modified and improved from conventional impedance fuel cell models. This modeling method provides a nonlinear electrical circuit mathematically derived from a particular group of impedance models. These impedance models were mapped from the electrochemical impedance spectra measured point-to-point along the polarized curve of the particular fuel cell. The derived equivalent circuit is composed of lumped nonlinear electrical circuit elements that include resistors, capacitors, and inductor. The resulting nonlinear circuit fuel cell models can have an impedance equivalent to the particular fuel cell in a wide operating range. The model also provides a good approximation of the static and transient behaviors of the fuel cell under various load changes.

2. The method for modeling

This modeling method is derived from the impedance modeling of fuel cell. Impedance fuel cell model is a linear electric circuit mapped from the impedance spectrum of the fuel cell operating in certain stationary operating condition. While changing the stationary fuel cell operating current or voltage, a series of impedance models can be obtained by fitting these impedance spectra, respectively. In principle, if the profile of the impedance spectrum changes smoothly, the impedance models can be mapped by the same type of equivalent circuit, and the values of each element in the impedance models can be fitted by a function of cell current or cell voltage. This function expresses the values of the linearized element related to its operation conditions. The linearized element is called a pseudo-electric element in this paper. Based on the definition of electrochemical impedance and the theory of nonlinear electric network, eventually, the expression of the relative nonlinear electric element can be mathematically derived from the function of the pseudo-electric element.

Because electrochemical impedance spectra of the target fuel cells present their proprietary nature, the equivalent electrical circuit fuel cell model obtained by this modeling method should be dependant on the type of the target fuel cell. In this paper, a direct methanol fuel cell (DMFC) was used as an example of the target fuel cell to be modeled by using this modeling method.

2.1. Experimental

A commercial membrane electrode assembly (MEA) (LIM005DA117EC, Lynntech Industries Ltd.) with 4.0 mg cm^{-2} PtRu black loading on the anode and 4.0 mg cm^{-2} Pt black loading on the cathode was used in this experiment. The MEA was inserted between 5-cm^2 single-cell endplates (LIE005TCHO, Lynntech Industries Ltd.) for testing. 1 M methanol aqueous solution was used as the fuel at the anode and was cycled by a chemical pump at the rate of 24 ml min^{-1}. The formed DMFC cell and the reservoir of methanol aqueous solution were set in an electric stove and the temperature controller on the stove was set at 60 °C during the entire testing. Room temperature air flux at 20 psi was inputted into the cathode endplate. A Solartron electrochemical workstation (SI-1280B, Solartron) was connected to the electric terminals on both anode and cathode side of the DMFC to measure the polarization curve and electrochemical impedance spectrum of the target DMFC. The detailed experimental setup and operating conditions are the same as those in our previous experimental research [6].

2.1.1. Polarization curve

The steady-state performance, or polarization curve, of the fuel cell with commercial MEA was measured by scanning the cell voltage at the rate 1 mV s^{-1}. The curve is approximately a linear line at a current greater than 0.03 A cm^{-2}, which indicated that mass transport limitations can be eliminated in the present running condition.

2.1.2. Electrochemical impedance spectra

The same experimental setup was used to measure the electrochemical impedance spectrum of DMFC. The impedance measurements were executed on various bias cell voltages from

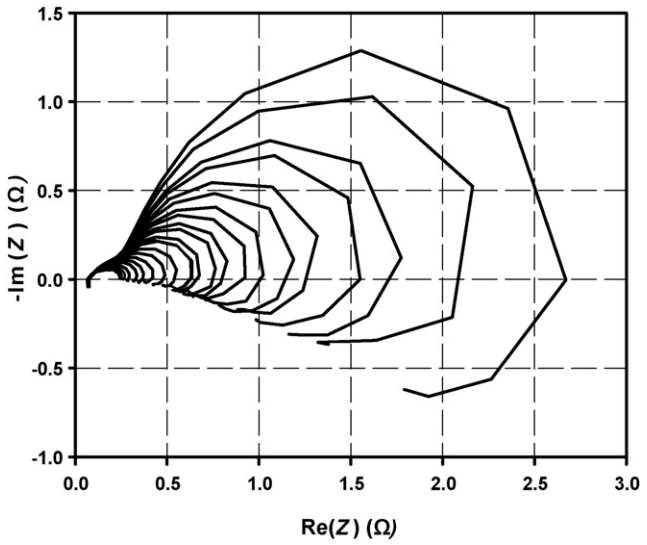

Fig. 1. Impedance spectra of the target DMFC from the outer most to inner most loops were measured at the cell voltage ranged from 0.5 to 0.1 V, respectively, and with voltage increment of 0.01 V between each neighboring impedance spectrum.

0.5 to 0.1 V (it covers the partial kinetic region and ohmic region of the polarization curve in our experimental condition) and frequency range from 0.01 to 20 kHz with 10 steps per logarithmic decade. The applied potential alternating amplitude V_m is 10 mV for the entire measurements. The electrochemical impedance spectra of the DMFC are displayed in Fig. 1. All these electrochemical impedance spectra have similar profiles and vary gradually with the change in the bias voltage or current.

2.2. Equivalent circuit and fundamental equations

2.2.1. Equivalent circuit for modeling of the impedance behaviors

The fundamental equivalent circuit for modeling of impedance behaviors of the target DMFC is shown in Fig. 2. The equivalent circuit consists of two sub-circuits: the first sub-circuit is a linear electrical circuit that may consist of a resistor only, or several resistors and/or resistor–capacitor pairs connected in serial, or other equivalent circuit; the second sub-circuit is a specific RCL circuit that was first theoretically predicted by Harrington and Conway [7] for hydrogen evolution reactions (HERs) with adsorbed intermediates, and then Mueller et al. [8] which proved to be in well agreement between this RCL equivalent circuit and the anodic impedance behavior of the DMFC. In their experiments, the DMFC was operated at very high fuel flow rate. Presently, Hsu et al. [9] phenomenally developed this RCL equivalent circuit by replacing the conventional capacitor with a constant-phase element (CPE) and incorporating two resistive and/or resistive–capacitive components for membrane and anode–membrane interface, respectively. Their equivalent circuit fitted the anodic impedance behavior of DMFC very well even in high frequency range. The equivalent circuit of Fig. 2 is based on and similar to the above equivalent circuits. However, the equivalent circuit of Fig. 2 represents the impedance of the entire DMFC, not only the anode electrode of DMFC. Because of the similarity of our equivalent circuit model and the above mentioned circuit models for anode of DMFC, this approach implies that the cathodic impedance of DMFC was also represented by resistive–capacitive pairs in this study. These resistive–capacitive pairs have much smaller impedance compared to the anodic impedance in the low frequency region or their cut-off frequency at over several tens of hertz. They mainly express the impedance behaviors of fuel cell in the high frequency region. The effects of air stoichiometric rate on cathode impedance and the methanol stoichiometric rate on anode impedance have been studied by several research groups [8,11,18]. In their experimental results, the high methanol stoichiometric rate increases anode impedance, contrarily high air stoichiometric rate decreases cathode impedance. These effects may illustrate the reason why the impedance of the entire DMFC is similar to the impedance of the anode operating in the condition of high methanol stoichiometric rate. The cathode impedance is most possible negligible compared to the anode impedance in our experimental condition. The difference between static voltage drops on anode and cathode electrodes of the DMFC in the same experimental condition had been measured and discussed previously [6]. The equivalent circuit in Fig. 2 was used to model the entire DMFC is because it fits the impedance of entire DMFC obtained in our experiments. Different or modified equivalent circuit might be better for modeling the entire DMFC operating in other specific conditions.

2.2.2. Equations for steady-state performance

The fuel cell polarization curve can be fitted by several empirical equations that are called performance equations of the fuel

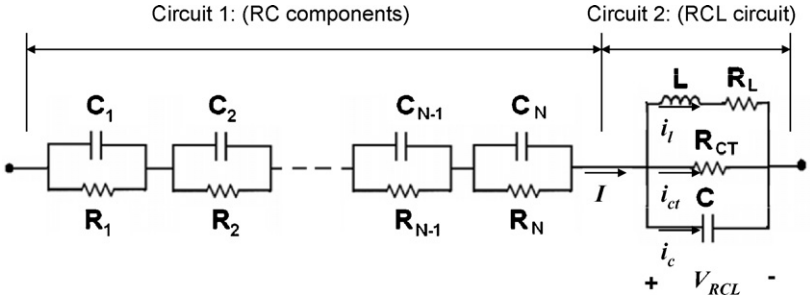

Fig. 2. The plot of the equivalent circuit for DMFC.

cell. The most basic performance equation is [1]:

$$V = V_{OCV} - A\ \ln\left(\frac{I}{I_0}\right) - R_{ohm}I - V_{CON} \quad (1)$$

where V is the cell voltage, I is the cell current, I_0 is the exchange current, A is the Tafel parameter for oxygen reduction, and R_{ohm} represents the cell ohmic resistance. V_{OCV} in Eq. (1) represents the reversible open circuit voltage (OCV), and the remaining terms reflect the activation loss, ohmic loss and mass transport loss (V_{CON}), respectively. Among them, mass transport loss term can be eliminated in the condition of high gas flow rate at the cathode. In this condition, the performance equation can be simplified to

$$V = V_{OCV} - A\ \ln\left(\frac{I}{I_0}\right) - R_{ohm}I \quad (2)$$

Eq. (2) is the standard electrode performance equation. In the present study, the polarization curves obtained in our experiments fitted this equation very well. By fitting the polarization curve to the standard electrode equation, the values of the parameters V_{OCV}, A and R_{ohm} can be obtained. This equation will be used for the present modeling to validate the steady-state solution of the nonlinear circuit dynamic DMFC model.

2.2.3. Fundamental equations for dynamic response of the nonlinear equivalent circuit

The novel nonlinear electric circuit for DMFC (Fig. 2) has the simplified format in which the first sub-circuit is assumed to be a single linear or nonlinear resistor R_t. This is an approximation that causes a deviation in the experimental impedance spectrum of the fuel cell in the high frequency region (higher than tens of hertz). However, our numerical study has proved that the profile of the fuel cell's high frequency impedance spectrum barely influences the transient behaviors of voltage overshoots and undershoots. This result can be understood by the fact that the overshoots and undershoots usually take over seconds to their equilibration levels. In the frequency domain, the Fourier transformation of the voltage overshoot or undershoot is a frequency function in which the high frequency (e.g. $f > 100$ Hz) components are very small and can be approximated as zero comparing with its components in the low frequency (e.g. $f < 100$ Hz) region. The impedances of the RC electric components replaced by single resistor R_t have a cut-off frequency over 100 Hz. In the frequency region much smaller than 100 Hz, these RC electric components work like pure resistors connected in series. Voltage overshoots and undershoots are the phenomena provoked by a low frequency prompt load change of fuel cell. Therefore, this approximation will not cause significant deviations when simulating the transient phenomena of voltage overshoots and undershoots. The elements in the RCL circuit are assumed to be nonlinear circuit elements. Under this assumption, the dynamic response of the nonlinear electric circuit model can be expressed as differential equations:

$$V = V_{OCV} - V_{RCL} - R_t(I)I \quad (3.1)$$

$$V_{RCL} = R_{CT}(i_{ct})i_{ct} \quad (3.2)$$

$$i_c = \frac{dq_c}{dt} = \frac{d}{dt}(CV_{RCL}) = \left[C(V_{RCL}) + V_{RCL}\frac{\partial C(V_{RCL})}{\partial V_{RCL}}\right]\left(\frac{dV_{RCL}}{dt}\right) \quad (3.3)$$

$$V_{RCL} = R_L(i_l)i_l + \frac{d}{dt}[L(i_l)i_l] = R_L(i_l)i_l + \left[L(i_l) + i_l\frac{\partial L(i_l)}{\partial i_l}\right]\left(\frac{di_l}{dt}\right) \quad (3.4)$$

$$I = i_{ct} + i_c + i_l \quad (3.5)$$

where V_{OCV} is the same parameters defined in Eq. (2), V and I are the voltage and current of the fuel cell, V_{RCL} is the voltage drop on the RCL circuit, and i_{ct}, i_c and i_l are the current via charge transfer resistor R_{CT}, capacitor C, and inductor L, respectively. The q_c is the charge stored in the capacitor.

2.2.4. Impedance of the equivalent nonlinear circuit

Fundamentally, the electrochemical impedance spectrum measurements are based on the small-signal perturbation approximation. The available commercial instruments measure impedance directly in the frequency domain by applying a small monochromatic voltage or current stimulus to the interface which is operating in a specific steady-state running condition, and measuring the phase shift and amplitude, or real and imaginary parts, of the resulting current at that frequency. For nonlinear electric circuit system, a monochromatic signal, one involving $\sin(\omega t)$, results in the generation of harmonics in the output. Both solid and liquid electrochemical systems tend to show strong nonlinear behavior when applied voltage or current are large. But as long as the applied potential difference amplitude V_m of the monochromatic voltage stimulus is less than the thermal voltage, $V_t = kT/e$, which is about 25 mV at 25 °C, it can be shown that the basic differential equations which govern the response of the system become linear to an excellent approximation [10]. Here k is Boltzmann's constant, T the absolute temperature, and e the proton charge. Note that, complex signals always split into their stationary and time perturbation parts in the equations for theoretical impedance.

The linearized differential equations for impedance spectrum of the circuit can be derived by applying the small-signal perturbation approximation to Eqs. (3.1)–(3.5) and eliminating high order perturbation terms. In these equations the steady-state conditions (V_{RCL}^0, I^0, $i_c^0 = 0$, i_{ct}^0 and i_l^0) have been used:

$$\Delta V = -\Delta V_{RCL} - \left[R_t(I) + \frac{\partial R_t(I)}{\partial I}I\right]|_{I=I^0}\Delta I = -\Delta V_{RCL} - R_t'(I^0)\Delta I \quad (4.1)$$

$$\Delta V_{RCL} = [R_{CT}(i_{ct}) + \frac{\partial R_{CT}(i_{ct})}{\partial i_{ct}}i_{ct}]|_{i_{ct}=i_{ct}^0}\Delta i_{ct} = R_{CT}'(i_{ct}^0)\Delta i_{ct} \quad (4.2)$$

$$\Delta i_c = \left[C(V_{RCL}) + V_{RCL}\frac{\partial C(V_{RCL})}{\partial V_{RCL}}\right]|_{V_{RCL}=V^0_{RCL}}\frac{d}{dt}(\Delta V_{RCL})$$
$$= C'(V^0_{RCL})\frac{d}{dt}(\Delta V_{RCL}) \quad (4.3)$$

$$\Delta V_{RCL} = \left[R_L(i_1) + i_1\frac{\partial R_L(i_1)}{\partial i_1}\right]|_{i_1=i^0_1}\Delta i_1 + \left[L(i_1) + i_1\frac{\partial L(i_1)}{\partial i_1}\right]|_{i_1=i^0_1}\left(\frac{d\Delta i_1}{dt}\right)$$
$$= R'_L(i^0_1)\,\Delta i_1 + L'(i^0_1)\left(\frac{d\Delta i_1}{dt}\right) \quad (4.4)$$

$$\Delta I = \Delta i_{ct} + \Delta i_c + \Delta i_1 \quad (4.5)$$

where the R'_t, R'_{CT}, R'_L, C' and L' are constants related to the specific steady-state conditions; however, they are the pseudo-constant electric elements if the correlative elements are nonlinear elements. They are called as pseudo-electric elements in this paper. After applying Fourier transform to these linearized time differential equations (4.1)–(4.5), they become linear algebra equations allowing the impedance spectrum of the nonlinear circuit to be easily obtained. Note that all the parameters of the nonlinear components of Eqs. (4.1)–(4.5), contribute to the pseudo-electric elements and can be expressed in the same equation as

$$A' = \left[A(x) + \frac{dA(x)}{dx}x\right]|_{x=x_0} \quad (5)$$

where the $A(x)$ represents the nonlinear parameter of $R_{CT}(i_{ct})$, $R_L(i_l)$, $R_t(I)$, $C(V_{RCL})$ and $L(i_l)$, and x represents the variables of i_l, i_{ct}, I and V_{RCL}. If $A'(x)$ is a continue function of variable x, this equation can also be converted into a differential equation:

$$\frac{d[xA(x)]}{dx} = A'(x) \quad (6)$$

It has the general solution:

$$A(x) = \frac{\int A'(x)dx + c}{x} \quad (7)$$

where c is an integral constant. The function $A'(x)$ is the expression of pseudo-electric element and it can be measured by electrochemical impedance spectroscopy in the present study. The $A(x)$ derived by Eq. (7) is the expression of the nonlinear electric element in the nonlinear equivalent circuit for the fuel cell.

2.3. Modeling

2.3.1. Impedance models mapped from impedance spectra

ZView software (Scribner Associates) was used to model the impedance behavior of the DMFC with the linear equivalent circuit in Fig. 2. ZView fits the selected electric circuit to experimental impedance spectrum date and displays the value of the parameter of each electric circuit element in the best-fitting condition. The fitting was carried out between 0.01 Hz and 10 kHz. The errors of the modeling parameters are within 1% for the impedance spectra of the DMFC (Fig. 1).

The measured total pseudo-resistance $\Re'_t(I^0)$ of the first sub-circuit and the pseudo-capacitance of the specific RCL circuit $C'(I^0)$ are shown in Fig. 4. The value $\Re'_t(I^0)$ slowly decreases with increasing of cell current I^0. In the research by Mueller and Urban [11], a medium frequency arc within 1 kHz to 1 Hz frequency region was reported for both the anode and cathode impedance spectrum of DMFC, which decreases with increasing cell current. In the present study, the cut-off frequency of all the RC components in the first sub-circuit of the impedance model are higher than 100 Hz, however, the medium frequency arc in our experiment was not observed, and the fitting parameter of each resistor in the first sub-circuit varies randomly. The medium frequency arc is a mass-transport related semicircle, and it can be eliminated by using very high fuel flow rates [8]. At 50 mA cm^{-2}, the stoichiometric flow rate of 1 M methanol is 3 ml min^{-1} [16], which is one-eighth of the flow rate of 1 M methanol used in our experiments. Hence, the medium frequency arc was mostly eliminated and the variation of the pseudo-resistances was due to the measuring deviations. The pseudo-resistor $\Re'_t(I^0)$ is approximately a constant in the present study. This is only an assumption or simplification to fit this equivalent circuit model to the empirical fuel cell performance equation (2) in the follow modeling. This approximation should be acceptable as long as the empirical equation (2) is available.

The value of the measured pseudo-capacitance $C'(I^0)$ varies slightly around 0.9 C. It can also be approximated as a constant within our measurement precision, and then its related capacitive element is a constant element based on Eq. (7). The measured capacitance is much larger than the double-layer capacitance of the catalyst. However, it is in the range of the capacitance observed by Mueller et al. [8] from their experimental research on impedance spectroscopy of DMFC. In principle, this capacitance should include both the double-layer capacitance of catalyst and the Faradic pseudo-capacitance due to methanol oxidation on the surface of catalyst. The constant value of capacitor is widely used to express the double-layer capacitance but not the Faradic pseudo-capacitance due to methanol oxidation. In research by Mueller's el al. [8], the capacitance $C'(I^0)$ is believed to be in the order of 0.1–1.0 F cm^{-2}, depend on parameters such as current density. However, this conclusion was mentioned as known result and no experimental conditions and data had been listed in the literature. Our experimental result implies that the capacitance $C'(I^0)$ is most possible a slow varying valuable of current density when the DMFC operate in the condition of using very high fuel flow rates. However, the constant approximation should be acceptable in fuel cell modeling because this approximation has been widely applied to mathematical or empirical fuel cell models in published literatures [12,13]. In those fuel cell models, a constant double-layer capacitance was phenomenally imported and its value was much larger than the double-layer capacitance of the catalyst materials. This approximation of constant capacitance will also be used in our

model as a special case, but it is not the necessary condition in the present modeling method.

The other pseudo-elements $\Re'_{CT}(I^0)$, $\Re'_{L}(I^0)$, and $L'(I^0)$ in the specific RCL circuit revealed obvious nonlinearity and their values dramatically decreased while increasing the cell current. All of these values are approximately inversely proportional to the cell current of I^0. The products of cell current and the value of each pseudo-element are approximately constants or linear lines (Fig. 4). However, the deviation of the constant of these products becomes large when the fuel cell running in large cell current. The instability of the low frequency impedance of the DMFC is increased while the DMFC running in the condition of large cell current. One of the reasons is believed to be the increased humidification of the cathode electrode [14]. In the condition of large cell current, the water generation is not negligible and it increases the humidification of the surface of the cathode electrode. The phenomena of flooding was also observed in our experiment when the DMFC operating in the condition of cell current over 200 mA cm^{-2} and air flux less than 10 psi. The humidity change of the cathode during modeling process will break the conservation condition of the target fuel cell. In this case, fully electrical modeling of fuel cells is not the proper and suitable method to modeling of fuel cells. Another possible reason for this deviation may be a kind of modeling deviation. In principle, the equivalent impedance of the fuel oxidation should be distributed in the body of the catalyst layer. The micro-homogeneous structure has not been considered in the discrete equivalent electric circuit model. Recently, a transmission line fuel cell model has been established for DMFC [17]. Based on this model, the impedance spectrum broadening, a deviation comparing with that of our discrete equivalent electric circuit model, in low frequency (<100 Hz) has been found when the DMFC operating under large cell current condition. In this condition, the ohmic resistance of the catalyst layer is bigger than the equivalent impedance of the RCL circuit. This will cause the obvious deviation between the impedance spectra obtained from the transmission-line model and discrete electric circuit model. This kind of modeling distortion will be described and published in a separate article.

2.3.2. Numerical solution of the nonlinear equivalent circuit

The nonlinear element is derived using Eq. (7) by transforming the pseudo-electric element experimental data in Fig. 1 to a function of local variable (e.g. the current through the element or the voltage across the element). The local variable can be solved from the perturbation equations. (4.2)–(4.5) under steady-state running condition. In this condition, Eqs. (4.2)–(4.5) present the perturbation equations of a linearized pure resistive circuit network. It can be expressed in a matrix algebra formula:

$$\begin{bmatrix} 1 & 1 & 1 & 0 \\ R'_{CT}(i^0_{ct}) & 0 & 0 & -1 \\ 0 & 1 & 0 & 0 \\ 0 & 0 & R'_{L}(i^0_{l}) & -1 \end{bmatrix} \begin{bmatrix} \Delta i_{ct} \\ \Delta i_{c} \\ \Delta i_{l} \\ \Delta V_{RCL} \end{bmatrix} = \begin{bmatrix} \Delta I \\ 0 \\ 0 \\ 0 \end{bmatrix} \tag{8.1}$$

The valuables Δi_{ct}, Δi_c, Δi_l and ΔV_{RCL} can be generally obtained as the linear functions of ΔI. However, the above equations are still not suitable for deriving the local variables because the unknown matrix coefficients $R'_{CT}(i^0_{ct})$ and $R'_{L}(i^0_{l})$. Fundamentally, the values of the locale valuables can be determined if the total current or total voltage is known in an electric circuit network running in static conditions. In static conditions, the matrix coefficients $R'_{CT}(i^0_{ct})$ and $R'_{L}(i^0_{l})$ can be equivalently expressed as functions of I^0, which are $\Re'_{CT}(I^0)$ and $\Re'_{L}(I^0)$. The transformation can be mathematically expressed as, for example, $\Re'_{CT}(I^0) = R'_{CT}(T_{ct}I^0)$. T_{ct} is the linear or nonlinear transformation operator ($i^0_{ct} = T_{ct}I^0$). $\Re'_{CT}(I^0)$ and $\Re'_{L}(I^0)$ are numerical functions that can be obtained by fitting the electrochemical impedance spectra of the target fuel cell. The expression of the solvable equation (8.1) are

$$\begin{bmatrix} 1 & 1 & 1 & 0 \\ \Re'_{CT}(I^0) & 0 & 0 & -1 \\ 0 & 1 & 0 & 0 \\ 0 & 0 & \Re'_{L}(I^0) & -1 \end{bmatrix} \begin{bmatrix} \Delta i_{ct} \\ \Delta i_{c} \\ \Delta i_{l} \\ \Delta V_{RCL} \end{bmatrix} = \begin{bmatrix} \Delta I \\ 0 \\ 0 \\ 0 \end{bmatrix} \tag{8.2}$$

After replacing the perturbation marker Δ by the differential sign d, the solution of Eq. (8.2) is a group of differential equations, then the stationary local variable can be derived by integrating the valuable of cell current I^0:

$$i^0_{ct} = \int_0^{I^0} \frac{\Re'_{L}(x)}{\Re'_{CT}(x) + \Re'_{L}(x)}\,dx \tag{8.3}$$

$$i^0_{l} = \int_0^{I^0} \frac{\Re'_{CT}(x)}{\Re'_{CT}(x) + \Re'_{L}(x)}\,dx \tag{8.4}$$

$$i^0_{c} = 0 \tag{8.5}$$

Mathematically, all of the local variables can be solved as equations of cell current or voltage. By using these equations, the measured pseudo-elements then can be transferred to functions of their local variables. Finally, we can obtain the expression from Eq. (7) for each nonlinear element in the equivalent circuit.

The expression of each pseudo-element is generally a numerical function mapped from experimental data. Therefore, the derived nonlinear function of each electric circuit element is a numerical function. Using this numerical function, it is hard to simulate the transient phenomena of the fuel cell and separate the modeling deviation from measurement errors.

2.3.3. Approximated analytical solutions of the nonlinear equivalent circuit

In the present study, linearity or the inverse proportional property of the measured pseudo-elements (Figs. 3 and 4) have been used to obtain an approximated analytical solution of the nonlinear equivalent circuit for DMFC. The experimental results of the pseudo-elements are a function of cell current I^0 can be approximately expressed as

$$\Re'_{CT}(I^0) = \frac{A_{CT}}{I^0} \tag{9.1}$$

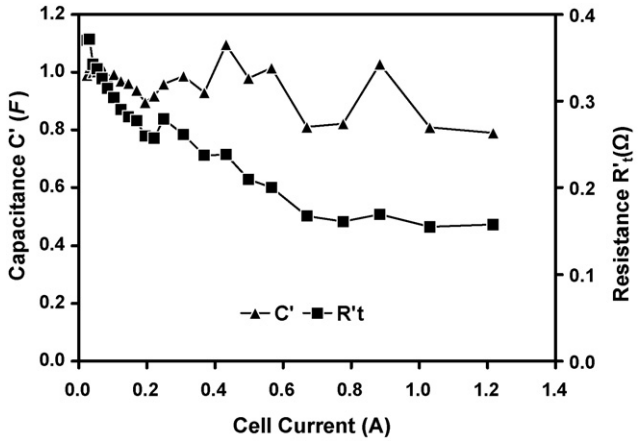

Fig. 3. The C' and $\Re'_t$ denote the parameters $C'(I)$ and $\Re'_t(I)$ mapped from the impedance spectra of the target DMFC obtained in different electrical operating conditions.

$$\Re'_L(I^0) = \frac{A_L}{I^0} \tag{9.2}$$

$$L'(I^0) = L_0 + \frac{B_L}{I^0} \tag{9.3}$$

$$C'(I^0) = C_0 \tag{9.4}$$

$$\Re'_t(I^0) = R_{ohm} \tag{9.5}$$

where A_i (i = L, CT), B_L, C_0, R_{ohm} and L_0 are constant parameters. Since these parameters are basically the experimental data, they can be determined by a group of impedance fuel cell models mapped from electrochemical impedance spectra of fuel cell.

These pseudo-elements can be transferred to functions of their local variables by solving these local variables from the perturbation equations (4.1)–(4.5) under steady-state condition, such as in Eqs. (8.1)–(8.5). It can be obtained

$$i^0_{ct} = \frac{A_L I^0}{A_{CT} + A_L} = \frac{I^0}{\alpha_{CT}} \tag{10.1}$$

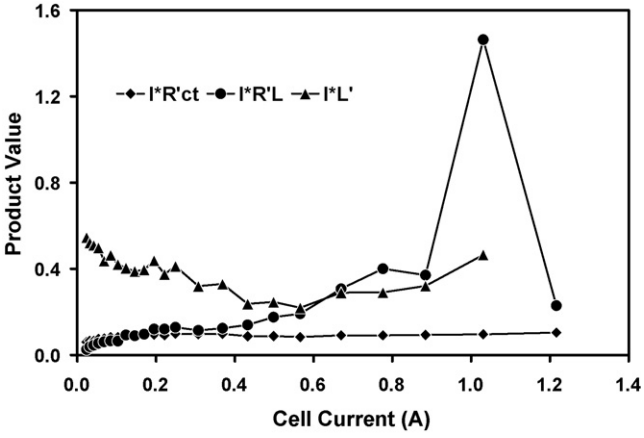

Fig. 4. The IR'_{CT}, IR'_L and IL denote the products of cell current I and the elements $\Re'_{CT}(I)$, $\Re'_L(I)$ and $L(I)'$, respectively, which are mapped from the impedance spectra of the target DMFC obtained in different electrical operating conditions.

$$i^0_l = \frac{A_{CT} I^0}{A_{CT} + A_L} = \frac{I^0}{\alpha_L} \tag{10.2}$$

$$i^0_c = 0 \tag{10.3}$$

where two new parameters α_i (i = L, CT) are defined

$$\alpha_{CT} = \frac{A_{CT} + A_L}{A_L} \tag{10.4}$$

$$\alpha_L = \frac{A_{CT} + A_L}{A_{CT}} \tag{10.5}$$

The proportional relation between stationary cell current I^0 and the branch current i^0_{ct} or i^0_l is the result based on the above approximation. This relation is only available when the fuel cell is running on static load.

After obtaining the expressions of the pseudo-elements as a function of their individual local electrical variables by substituting Eqs. (10.1)–(10.3) into Eqs. (9.1)–(9.5), the nonlinear function of the electrical elements in the equivalent fuel cell model can be finally derived by using Eq. (7) with the obtained local variable a function of the pseudo-elements. The final solutions are

$$R_{CT}(i_{ct}) = A_{CT} \frac{\ln(\alpha_{CT} i_{ct}/I_0)}{\alpha_{CT} i_{ct}} \tag{11.1}$$

$$R_L(i_l) = A_L \frac{\ln(\alpha_L i_l/I_0)}{\alpha_L i_l} \tag{11.2}$$

$$L(i_l) = L_0 + B_L \frac{\ln(\beta_L \alpha_L i_l/I_0)}{\alpha_L i_l} \tag{11.3}$$

$$C = C_0 \tag{11.4}$$

$$R_t = R_{ohm} \tag{11.5}$$

where the parameter I_0 comes from the integral constant of Eq. (7), the parameter β_L is a non-zero constant. Because the dynamic response and impedance spectrum are only related to the pseudo-inductance of $L'(i_l)$, β_L can be normalized to one in the following simulation and model validation.

In Eqs. (11.1)–(11.3), all of the constant parameters except the I_0 are the same constant parameters as those were determined in steady-state equations. That means, so far as the approximate equations (9.1)–(9.5) are available, A_i, α_i (i = L, CT), B_L and L_0 should be the constant parameters and available to the equivalent circuit model for simulating of the fuel cell running on dynamic load.

2.4. Model validation

2.4.1. Static model

Based on the derived equivalent circuit fuel cell model, its total resistance of the model in steady-state running condition is R_{ohm} plus R_{RCL}. R_{RCL} is equal to the pair of R_{CT} and R_L connected in parallel. Applying Eqs. (11.1) and (11.2) to Eq. (3.1), the equivalent resistance can be easily obtained by Ohm's

law. Then, the polarization of the target DMFC is

$$V = V_{OCV} - A \ln\left(\frac{I}{I_0}\right) - R_{ohm} I \tag{12.1}$$

$$A = \frac{A_{CT} A_L}{A_{CT} + A_L} \tag{12.2}$$

where the integral constant I_0 can be understood as the exchange current in fuel cell performance equation (2), it was normalized as 1 A in the following simulation. Parameter A is the Tafel coefficient which is related to the experimental parameters A_{CT} and A_L based on Eq. (12.2). This equivalence indicates three very important results: (1) the total resistance in first sub-circuit of our model is the cell ohmic resistance R_{ohm} of the target DMFC; (2) the RCL circuit mainly describes the fuel oxidation at the anode of the target DMFC and its steady-state voltage drop is the Tafel term in Eq. (2); (3) the cathode impedance is merged to the cell ohmic resistance term and/or partially to the RCL circuit in the absence of mass transport limitation.

Because the static fuel cell model is a steady-state solution of our dynamic fuel cell model, the experimental results for transient behaviors of the DMFC were used to validate the static fuel cell model (Fig. 6). Each static cell voltage was derived by averaging the static cell voltages after the DMFC reached equilibrium. The experimental results are plotted in Fig. 5. A simulation result of the static model is also plotted out in this figure to compare with the experimental results. The parameters for simulating of the static model are list in Table 1, which are selected from the polarization curves measured during the entire experiments.

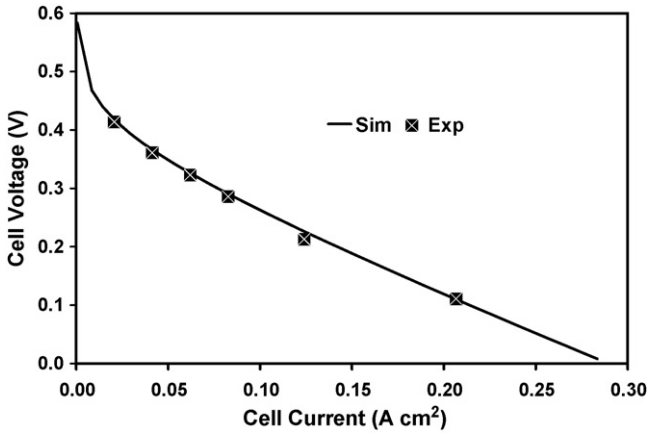

Fig. 5. Experimental and simulation results of the steady-state performance of the DMFC.

2.4.2. Dynamic model

The completed electrical fuel cell model has been implemented in MATLAB/SIMULINK by applying Eqs. (3.1)–(3.5).

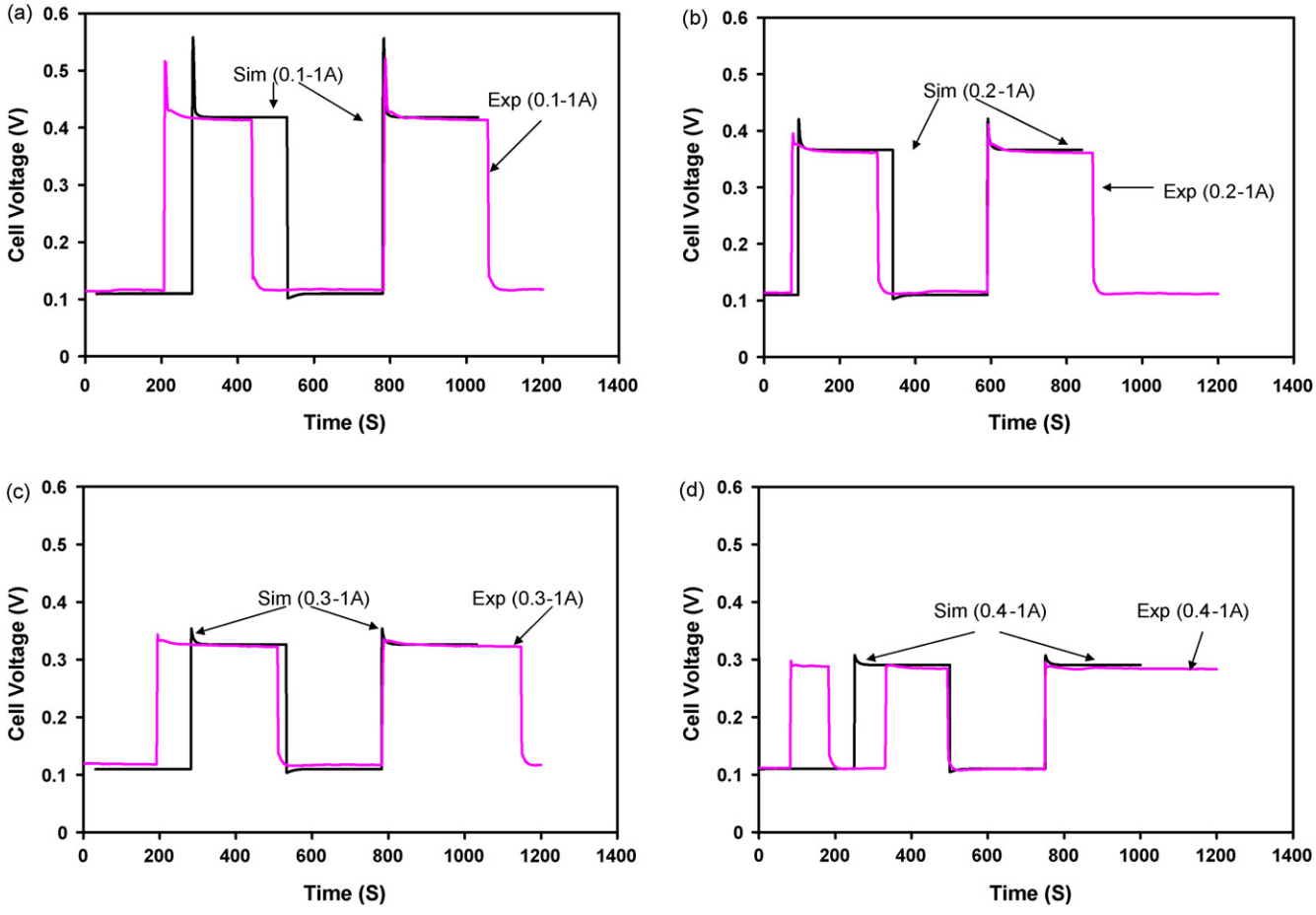

Fig. 6. Comparison of the experimental (Exp) and simulation (Sim) transient behaviors of the DMFC operated under square current pulses: (a) the upper and low levels are 1 and 0.1 A, (b) the upper and low levels are 1 and 0.2 A, (c) the upper and low levels are 1 and 0.3 A and (d) the upper and low levels are 1 and 0.4 A.

Table 1
Parameters for the nonlinear equivalent circuit for modeling of DMFC (I_0 = 1 A)

Data type	R_{ohm} (Ω)	A (V)	A_L (V)	A_{CT} (V)	C (F)	L_0 (H)	B_L (H A)	V_0 (V)
Experimental								
I–V curve	0.236–0.244	0.027–0.030	/	/	/	/	/	0.35–0.40
EIS	0.16–0.40	0.02–0.09	0.026–0.40	0.066–0.10	0.8–1.1	−0.35	0.6	/
Simulation	0.24	0.04	0.2	0.05	1.0	−0.35	0.6	0.35

The simulation results were compared with the transient behaviors of the target DMFC operating under square current pulses with the same upper current level of 1 A and various low current levels. The comparisons between simulation and experimental results are displayed in Fig. 6.

During measuring of the electrochemical impedance spectra of the target DMFC, the polarization curve of the target DMFC had been monitored. The variations of the parameters V_{OCV}, A and R_{ohm} obtained by fitting these polarization curves are listed in Table 1. The variations of the experimental parameters A_{CT}, A_L, C and R_{ohm} mapped from electrochemical impedance spectra (EIS) of the target DMFC (Figs. 1 and 5) have also been listed in Table 1. The EIS parameter A was derived from the EIS data of A_{CT} and A_L by using Eq. (12.2). The parameter L_0 and B_L was directly obtained by fitting the curve of the product $I^0L'(I^0)$ (in Fig. 4) to a linear function based on Eq. (9.3).

The approximated analytical equivalent circuit model expressed in Eqs. (11.1)–(11.5) was used in the simulation. To determine the constant parameters of the present dynamic fuel cell model, a strategy had been used. Because the measured polarization curves are relatively more stable than the EIS experimental data, the parameters V_{OCV}, A and R_{ohm} obtained from the polarization curve fitting method are preferred to be referred. The parameters A_{CT} and A_L are selected within the range of EIS data while keeping the selected parameter A constant using Eq. (12.2). The EIS parameters L_0 and B_L were directly used in the simulation. All of the parameters selected for our simulation are also listed in Table 1.

In Fig. 6, the numerical transient behaviors of the DMFC at cell current 1 A are obviously deviated from the relevant experimental results. Based on our model, the transient behavior should be an undershoot after the cell current step change to 1 A. No undershoot has been observed in the relevant experimental results; however, the cell voltage varies slowly to its equilibrium state. In the experiments, when the cell current changes from 0.1 to 1 A, a typical response pattern was observed: a tiny undershoot after a prompt response to an intermediate value of voltage, followed by a slow response to a lower steady voltage (Fig. 6a). This kind of phenomena had also been reported in literature [15].

In our experimental conditions, the amplitude of small undershoot and relaxation time of the slow response were increased with increasing the flux of dried air at the cathode side. Reducing the flux of dried air was able to reduce the undershoot and slow varying time, but also caused instability of the fuel cell because of the flooding in the cathode surface. The undershoot and slow relaxation time decrease if the amplitude of cell step current change is reduced. In conclusion, this kind of modeling deviation occurs when DMFC is promptly alternating between two cell currents, one of them is in the high current level and the other is much smaller than the previous one.

Since the typical slow variation of the voltage is at the scale over 10 s, this characteristic time corresponds to the impedance spectrum at or below ∼0.01 Hz. This low frequency region is not well covered in conventional electrochemical impedance spectrum measurements. It is possible that the impedance spectrum of DMFC operating in high cell current has a specific structure in this low frequency region. The impedance fuel cell model presented by Mueller might be ineffective at the frequency below 0.01 Hz when the DMFC operating in the conditions of high cell current, constant temperature, constant concentration of methanol solution and constant air flow.

In physics, this modeling deviation is possibly due to the slow response of the humidity of electrodes of DMFC. In our fuel cell modeling, all of the parameters, excepting cell current and cell voltage, are assumed to be constants. The variation of these non-electric parameters during experiments is the fact that causes modeling deviation.

3. Conclusions

The modeling method demonstrated in this paper is a semi-empirical fuel cell modeling method. By using this method, a nonlinear equivalent electrical circuit dynamic fuel cell model can be mathematically derived from a specific group of impedance fuel cell models that are developed experimentally.

The obtained equivalent circuit for DMFC is similar to Mueller's impedance fuel cell model, but its lumped elements are basically nonlinear elements. The equivalent circuit includes lumped capacitors and resistors as well as a nonlinear inductor. Therefore, it can be used to simulate the transient behaviors of DMFC such as voltage overshoots or undershoots. The resulting nonlinear circuit fuel cell model can have an impedance equivalent to the particular fuel cell in wide electric operating ranges and provides a good approximation of the static and transient behaviors of the fuel cell under various load conditions. However, the specific equivalent circuit model for DMFC was obtained in the condition of no mass transport losses at anode and cathode. Mueller's impedance fuel cell model may not be valid in the presents of mass transport limitations [8,9]. The method demonstrated in this paper is not limited to Mueller's impedance fuel cell model and can also apply to other impedance models if the impedance model can fit a group of the impedance spectra of the fuel cell. The key points to have good modeling precision are a proper equivalent circuit for impedance fuel cell model and the stability of the fuel cell during the experiments.

Since this modeling method is independent of the type of fuel cells. It should be able to model other types of fuel cells (e.g. hydrogen PEM fuel cell, SOFC and others) that have a group of impedance fuel cell models mapped by the same equivalent circuit.

Acknowledgements

This research was partially supported by a FSU Cornerstone PEG Program and US Army CERDEC at Fort Monmouth, NJ.

References

[1] J. Larminie, A. Dicks, Fuel Cell System Explained, second ed., John Wiley & Sons, New York, 2003.
[2] W. Choi, J.W. Howze, P. Enjeti, J. Power Sources 157 (2006) 311.
[3] D. Yu, S. Yuvarajan, J. Power Sources 142 (2005) 238.
[4] R. Gemmen, P. Famouri, PEM fuel cell electric circuit model, in: Proceedings of the Power Electronics for Fuel Cell Workshop, 2002.
[5] C. Wang, N.H. Nehrir, IEEE Trans. Energy Convers. 20 (2) (2005) 442.
[6] Y. Wang, J.P. Zheng, Electrochem. Solid State Lett. 10 (1) (2007) B26.
[7] D.A. Harrington, B.E. Conway, Electrochim. Acta 32 (1987) 1703.
[8] J.T. Mueller, P.M. Urban, W.P. Hölderich, J. Power Sources 84 (1999) 157.
[9] N. Hsu, S. Yen, K. Jeng, C. Chien, J. Power Sources 161 (2006) 232.
[10] J. Ross Macdonald, Impedance Spectroscopy: Emphasizing Solid Materials and Systems, John Wiley & Sons, New York, 1987, p. 6.
[11] J.T. Mueller, P.M. Urban, J. Power Sources 75 (1998) 139.
[12] M. Eikerling, A.A. Konyshev, J. Electroanal. Chem. 475 (1999) 107.
[13] P.R. Pathapati, X. Xue, J. Tang, Renew. Energy 30 (2005) 1.
[14] R. Makharia, M.F. Mathias, D.R. Baker, J. Electrochem. Soc. 152 (2005) A970.
[15] P. Argyropoulos, K. Scott, W.M. Taama, J. Power Sources 87 (2000) 153.
[16] A. Oedegaard, C. Hentschel, J. Power Sources 158 (2006) 177.
[17] Y. Wang, J.P. Zheng, G. Au, E.J. Plochta, Proceedings of the 211th ECS Meeting, Chicago, IL, May 6–11, 2007.
[18] P. Piela, R. Fields, P. Zelenar, J. Electrochem. Soc. 153 (2006) A1902.